

Outdoor 3D Map Generation based on Planar Feature for Autonomous Vehicle Navigation in Urban Environment

Satoshi Kagami, Ryo Hanai, Naotaka Hatao and Masayuki Inaba

Abstract—This paper describes a 3D textured map generation method for autonomous vehicle in urban outdoor environment, where GPS signals can not be reached. Constructed map will be used for short cycle and accurate localization and for obstacle detection using onbody laser scanner.

In order to build dense 3D polygon map, planar feature of laser scanner input is extracted. They are associated and transformation matrices in between each scan point were iteratively solved. Aligned points were converted into texture mapped 3D polygons.

400x350[m] area in Univ. of Tokyo were scanned at 59 scan points, and 3D polygon map consists of 14M polygon were obtained. Experimental results of localization and autonomous path following two-wheeled inverted mobile robot PMR are shown.

I. INTRODUCTION

Recently, research on outdoor autonomous robots has become increasingly active, and a broad array of fundamental issues are under investigation. In the outdoor environment, GPS is mostly used for localization, however it is not so useful when sky is not widely opened so that satellites are not directly nor constantly visible, such as in urban city or under the trees.

In the indoor environment, laser scanner is widely used for 3DOF localization purpose from two dimensional map, however, this technique is not directly applicable for outdoor environment because in 3D environment, 6DOF localization is needed. For example, with 7 [deg] inclination causes 1.2[m] height difference in 10[m], and if map is two dimensional, this inclination makes localization impossible. Few degrees of inclination also may happen from vehicle posture changes, and this causes sensor looks at ground or air.

Therefore, 3D map together with 6DOF localization becomes important for outdoor terrain, where GPS is not able to use. Authors previously showed a online particle filter based 6DOF localization technique from 3D map [1].

So far, many 3D map building algorithms from multiple camera views have been proposed in computer vision field, (i.e. Structure from Motion). Those techniques basically consist of feature extraction, their association, and reconstruction. Factorization [2] is a tracking based approach, and bundle adjustment technique(ex. [3]) is introduced in order to optimize 3D structure and camera parameters. There are also sampling based approach by introducing Markov Chain Monte Carlo model [4, 5], or by Expectation Maximization method [6, 7]. Recently SIFT feature is widely used as for

a feature extraction [8]. This framework calculates reconstructed map together with camera parameters, however the map is basically sparse since original features are sparse.

On the other hand, 3D map building algorithms from many scans of laser scanner input have also been proposed, such as ICP [9, 10] and 3D SLAM methods [7, 11] by introducing MCMC. This framework calculates transformation matrices in between each scans, so that the resulted map becomes dense. However in natural environment, high frequency region such as tree leaves or grass exist and it is difficult to handle such a environment.

Therefore, in this paper, we propose a method to obtain large scale 3D map, by extracting planar features from multiple laser scanner input, to solve transformation matrices of each scans, by omitting high frequency regions in the scene. As a result, we can obtain dense 3D map, so that the map can also be used for obstacle detection.

II. 3D MAP GENERATION

A. 2D Laser Scanner

In this paper, we adopted Riegl LMS-Z420i as for a 2D laser scanner(Fig.1). This equipment is class 1 laser (eye safe) and it can measure 80 [deg] for elevation and 360 [deg] for azimuth at a time with maximum 0.01 [deg] resolution. Distance measurement is 1[mm] resolution and standard deviation of absolute measurement is 10[mm]. It can measure 350[m] with more than 10% reflection object.

One scan with 0.1 [deg] resolution causes 2.5M points (X, Y, Z, R, G, B and reflection power), and with 0.01 [deg] causes 250M points respectively.

As like other time of flight bases laser scanning equipment, this scanner also doesn't have remarkable distortion nor non-linear sensitivity from distance to a target. Therefore, in this paper we only estimate external parameter (i.e. transformation matrices) of each scan.

B. Marker based Calculation of Transformation Matrices

As for preliminarily experiment, total 80 times scan at 18 points(number 1-18 in Fig.2) were conducted in about 400 × 350[m], and about 100M points were obtained. As for load part, at least 15[cm] sampling were achieved by changing angular resolution.

At each scan, we put at least three (usually about five) of both following markers in the scene, and those markers are commonly seen from another scan: 1) reflective ball (5[cm] diameter) and 2) non-reflective white ball(15[cm] diameter).

Reflective markers are measured by 0.004[deg] resolution, and white markers are measured by 0.01[deg] resolution. As

Information and Robot Technology Research Initiative, Univ. of Tokyo, 7-3-1 Hongo, Bunkyo-ku, Tokyo, 113-8656, Japan



Fig. 1. LMS-Z420i Scanner Mounted on a Cart



Fig. 2. 59 Scan Points at Univ. of Tokyo

for white markers, hough transform is used to locate the center of the ball.

After finding center position of markers at each scan, those are associated and transformation matrices were solved by closed-form least square method [12]. There are multiple closed-loops arise, so in order to obtain global coordinates, iterative fitting of transformation matrices is adopted to minimize errors.

TOPCON GPT-9000A is utilized to locate scanner position by measuring reflective prism attached at top of laser scanner at each scan point. This equipment is also used to do optical land survey measurement at about 20 points in target area. We compared this result with the closest sampling point in previously obtained global coordinated scan points, and average error was about 5[cm].

Therefore, both reflective and white ball markers work well to obtain transformation matrices. However, there is two difficulties to use markers, the one is placement of marker balls that can be seen from another scans, and the other is measurement exactly around given markers in high resolution.

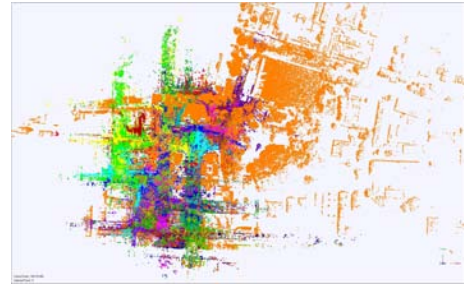


Fig. 3. Entire Scan Points after Aligning, Each Scan has Different Color



Fig. 4. Virtual View of Yasuda Tower by Omitting Adjacent Science Department Building No.1

C. Planar Feature based Calculation of Transformation Matrices

As a observation of scanning result, natural objects such as tree leaf, twig, bush, grass and so on, has higher frequency shape than laser scan. Therefore, low-pass filter is adopted for scanner result in order to obtain a low frequency shapes.

Obtaining feature that can be robustly found from the other view is required to associate then to calculate transformation matrices. In this paper, probabilistic planar feature extraction method is adopted proposed by Weingarten [13]. This method has three steps; 1) PCA based plane detection, 2) transformation of scan points, 3) uncertainty analysis using standard regression methods. After obtaining plane parameters, number of points on the plane, and its center of gravity are calculated.

Since there is no closed-form solution for planes to planes fitting, RANSAC is used iteratively pick up planes to find out transformation matrices by using non-linear least-square method [14]. In this case, transformation matrices are obtained globally, so that loop closing process shown in marker based method is not needed. Average error in between previously mentioned optical land survey points and estimated by this method was about 7[cm]. Therefore, this method can be used to obtain 3D map.

D. Polygon Map Generation

Since marker-less measurement is easy and fast, we scanned another 40 scan points (number 19–59 in Fig.2). After obtaining global transformation matrices and all scan data are shown in Fig.3. In this figure, each scan data has

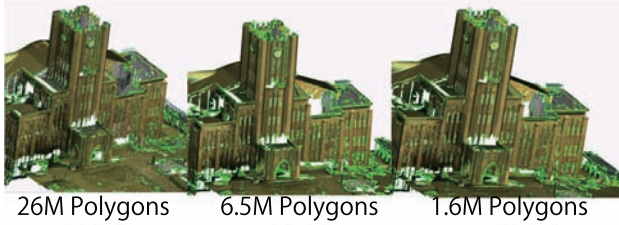


Fig. 5. Polygon Reduction Results in Low-Frequency Area

different color. Fig.4 shows a virtual view of Yasuda tower by omitting adjacent building(Science department building No.1). After this process, all data were about 1.5B points.

Then we sample among points to have at least 12.5[mm] distance to the other points, in order to reduce the number of data. The result was about 200M points. There are about 28% of high frequency data that comes from leaves and so on. Remaining 72% of low frequency data comes from building, load, and so on.

As for low frequency part, put polygons that have less than 12.5[mm] distance from points. Then color that was associated to each scan were texture mapped onto polygons with texel size of 12.5[mm]. Resulted number of polygons is same magnitude of number of points. However, using polygon reduction technique, we found that this low frequency region can be reduced into few %. Fig.5 shows 100%, 25% and 6% data of Yasuda tower.

As for high frequency region, polygon can't be directly mapped. Therefore, once the data is represented into volumetric kd-tree, and then converted into surface polygon. However, it is very dense and polygon reduction technique doesn't work with this data. Fig.6(above) shows 100%, 50% and 25% reduction of a large tree in front of Yasuda tower. Fig.6(below) shows a cut version, and it is seen that inside is also dense.

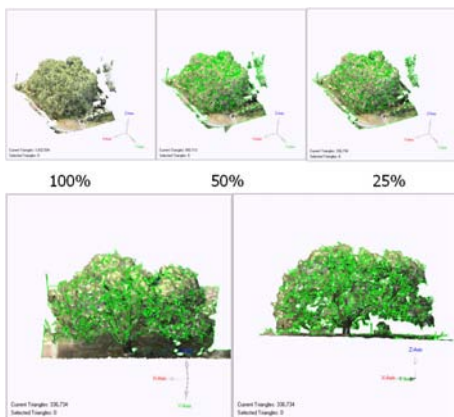


Fig. 6. Polygon Reduction Results in High-Frequency Area



Fig. 7. Rendering Result of 3D Polygon Map

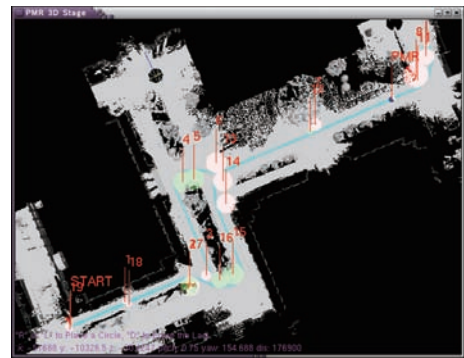


Fig. 8. Two-way Path from Eng. Bldg. No.2 to No.11

As for localization point of view, this high frequency region is not able to deterministically estimate the laser reflection. Therefore, in this paper, we use this high frequency region as uncertain area for localization.

Fig.7 shows a obtained polygon map combined high and low frequency area. It consists of about 15M polygons. This map can be rendered by using standard graphical hardware.

III. EXPERIMENT OF PATH FOLLOWING

A. Two-Wheeled Inverted Mobile Robot PMR

PMR(Personal Mobility Robot) [15] is a revised version of TOYOTA MOBIRO that was designed for single seated vehicle for urban terrain. Sensors (four Hokuyo UTM-30LX laser scanners, three omni-directional cameras and so on) and computer of PMR are improved from original MOBIRO. There are five DOF (seat slider, left and right swing arm, both wheels) and designed to keep seat upright even during rotating on a slope. Knee down mode is used in order to get in/out, and automatic transition in between inverted mode and knee down mode.

As for experiment, vehicle control method is proposed in [16].

Robot controller keeps PMR upright within about 5 [deg] even on the slope. Therefore, we cut off the polygon map

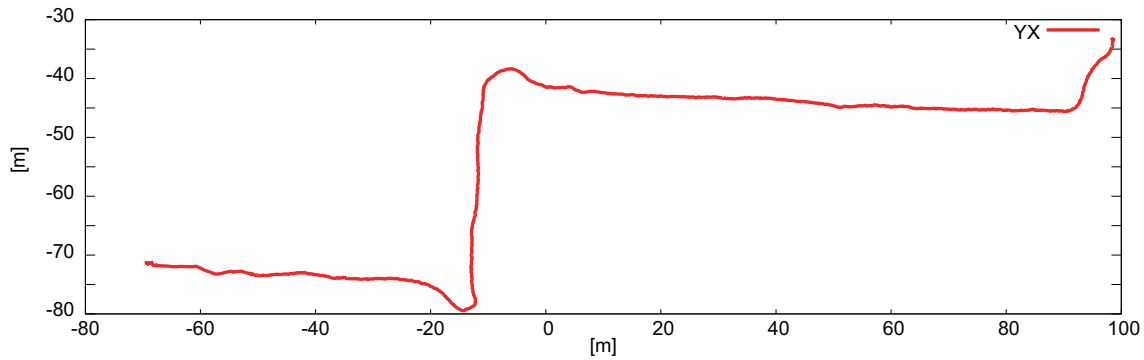


Fig. 10. Localization Result (XY) in PMR Experiment

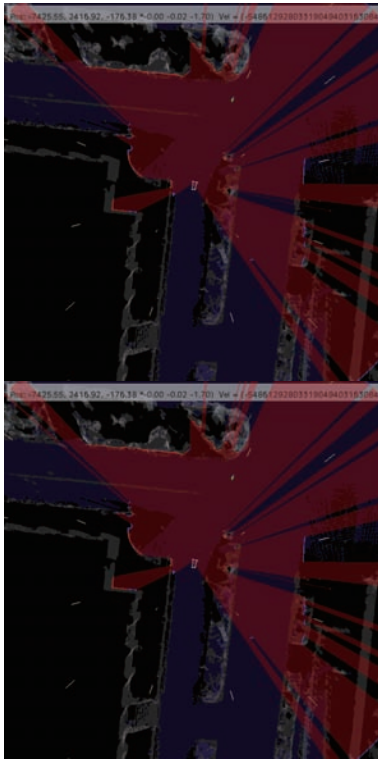


Fig. 9. Laser Scanner Input and Localization in PMR Experiment

more than 5[m] from the ground as well as high frequency regions. Remaining map contained about 1M polygons.

B. Localization Experiment

A two-way test course was set from engineering building No.2 to No.11 through both pedestrian way and load. Fig.8 shows the entire path. In the middle of the path contains one way load, so that the path differs in each other. Path length for one way is about 250[m]. This path contains 7[deg] inclination and 3[m] of height changes. In real environment, there are static and moving obstacles such as pedestrians, bicycles, cars and so on.

Initially localization experiment was conducted by manually driving PMR. Particle filter based 6 DOF Localization

method by using 1D (single line) laser scanner is proposed in [1].

Localization process is calculated by MacBookPro(G0Z0) that has Core2Duo-2.8GHz, 3GB memory, NVIDIA Geforce 9400M(256MB) graphics accelerator. With 1M polygons map, particle filter based localization with 100 particles works in 80-150[ms] cycles.

Fig.9 shows a laser scanner input together with matched laser point in red, while unknown objects in blue. At bottom figure of Fig.9 shows laser scan hits to the ground. Fig.10 shows a XY plot of one way run with about 1[m/s] speed and Fig.11 shows Z, roll, pitch and yaw at the same run.

After ten two-way run, error at the both-end were about 15[cm] in XY translation and about 12[deg] in yaw angle.

C. Autonomous Path Following

Path following method was proposed in [17]. This method adopts circle and line as a path component in order to guarantee time to travel of given path, so that robot can avoid moving obstacles such as pedestrian and bicycle. However, since it is not obvious to find out region that can run by PMR from given 3D map, in this paper, moving obstacle detection and prediction as well as moving obstacle avoidance is not adopted.

Instead, obstacle detection function stops PMR within 2[m] ahead. There is one laser scanner mounted horizontally, and two scanners are looking down to the ground 30[deg] from horizontal plane. [17].

Another course was set to examine a path following around engineering building No.6. Fig.12 shows the course. Tree becomes obstacles to the sky, so that ground can not be seen. Here GPS is completely not possible to use. The height difference of the course is more than 5[m].

Fig.13 shows a given and executed velocity while the experiment. In this experiment, 1.0[m/s] was given for translational speed. Fig.14 shows a localized and given path at the two corner. Fig.15 shows a PMR in motion in the experiment.

Combining localization, path following and vehicle control, autonomous path following were achieved with up to 1.2[m/s] translational speed and 0.5[m/s] rotational speed.

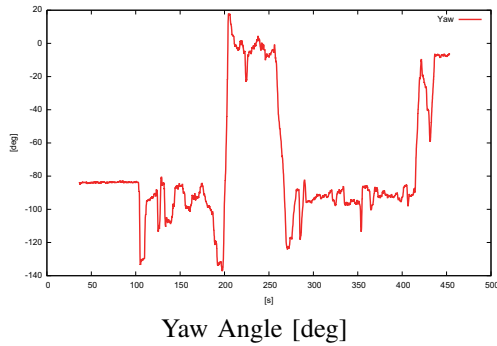
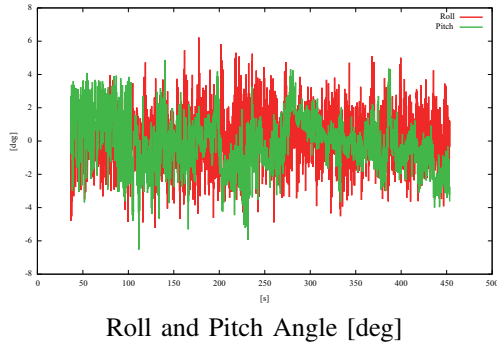
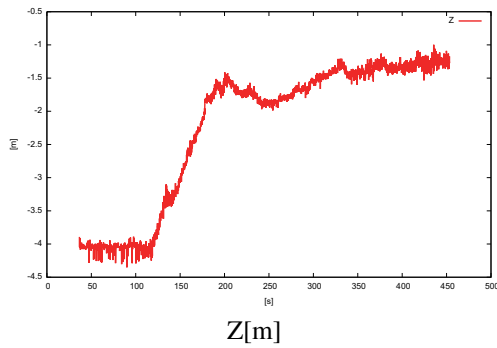


Fig. 11. Localization Result (Z, Roll, Pitch, Yaw) in PMR Experiment

IV. CONCLUDING REMARKS

This paper describes a planar feature based alignment of laser scanner inputs in order to build large scale outdoor 3D map that is used for localization and obstacle detection in mobile robot navigation.

In order to build dense 3D map for localization and obstacle detection, planar feature of laser scan input is extracted. They are associated and transformation matrices in between each scan point were iteratively solved. Aligned points were converted into texture mapped 3D polygons by omitting high frequency regions, then used for 6DOF localization from onbody 1D laser scanner. 400x350[m] area in Univ. of Tokyo were scanned at 59 scan points, and 3D polygon map consists of 14M polygons were obtained. Experimental results of localization and autonomous path following by PMR are also shown.

Particle filter based 6DOF localization with 1M polygon map works about 10[Hz] with accuracy of about 15[cm] in

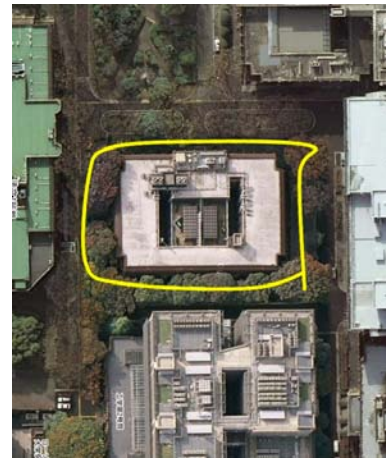


Fig. 12. Path Following Experiment Setup

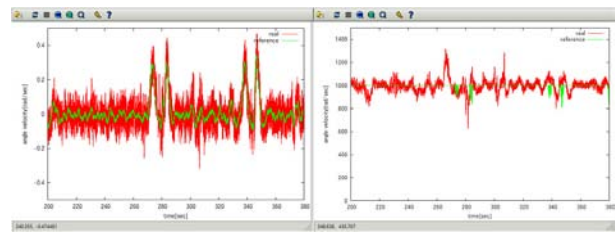


Fig. 13. Given and Executed Velocity in Path Following Experiment (Translational and Rotational)

XY translation and 12[deg] in yaw angle.

Next, autonomous navigation is our target. In order to achieve autonomous navigation, we need to find out regions that can run by PMR in both physical and manner (or rule) point of view.

We would like to integrate image based structure from motion together with laser scanner based map. Sparse map build by image based structure from motion is useful for just localization, and especially outdoor has enough features.

ACKNOWLEDGEMENT

This research is partly supported by Special Coordination Funds for Promoting Science and Technology, “IRT Foundation to Support Man and Aging Society”.

REFERENCES

- [1] S. Thompson, S. Kagami, and K. Nishiwaki, “Localisation for autonomous humanoid navigation,” in *Proceedings of 2006 6th IEEE-RAS International Conference on Humanoid Robots(Humanoids2006)*, December 2006, pp. 13–19.
- [2] C. Tomasi and T. Kanade, “Shape and motion from image streams under orthography: a factorization method,” *International Journal of Computer Vision*, vol. 9, no. 2, pp. 137–154, 1992.
- [3] B. Triggs, P. Mclauchlan, R. Hartley, and A. Fitzgibbon, “Bundle adjustment – a modern synthesis,” in *Vision Algorithms: Theory and Practice, LNCS*. Springer Verlag, 2000, pp. 298–375.
- [4] S. I. D. Forsyth and J. Haddon, “Bayesian structure from motion,” in *Proceedings of the International Conference on Computer Vision (ICCV)*, 1999, pp. 660 – 665.

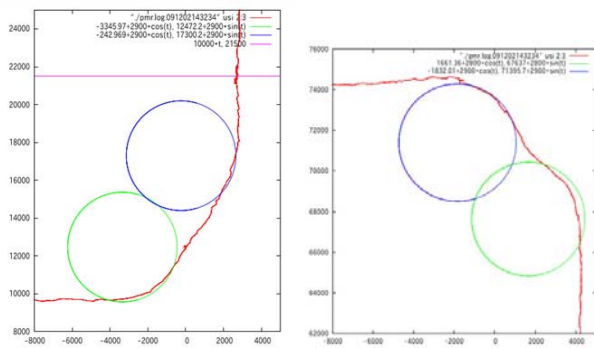


Fig. 14. Given and Localized Trajectories at the Corner

- [5] F. Dellaert, S. Seitz, C. Thorpe, and S. Thrun, "Structure from motion without correspondence," in *IEEE Computer Society Conference on Computer Vision and Pattern Recognition (CVPR '00)*, June 2000.
- [6] A. Kelly, O. Amidi, M. Bode, M. Happold, H. Herman, T. Pilarski, P. Rander, A. Stentz, N. Vallidis, and R. Warner, "Toward Reliable Off Road Autonomous Vehicles Operating in Challenging Environments," in *Proc. of 9th International Symposium on Experimental Robotics*, 2004.
- [7] M. Montemerlo and S. Thrun, "Large-Scale Robotic 3-D Mapping of Urban Structures," in *Proc. of 9th International Symposium on Experimental Robotics*, 2004.
- [8] M. Tomono, "3d object modeling and segmentation using edge points with sift descriptors," in *IEEE/RSJ International Conference on Intelligent Robots and Systems (IROS 2008)*, Sep. 2008, pp. 4195–4200.
- [9] O. Faugeras and M. Herbert, "The representation, recognition, and locating of 3-d objects," *International Journal of Robotics Research*, vol. 5, no. 3, pp. 27–52, 1986.
- [10] F. Stein and G. Medioni, "Structural indexing: Efficient 3-d object recognition," *IEEE Transactions on Pattern Analysis and Machine Intelligence*, vol. 14, no. 2, pp. 125–145, 1992.
- [11] A. Howard, D. F. Wolf, and G. S. Sukhatme, "Towards autonomous 3d mapping in urban environments," in *In Proceedings of the IEEE/RSJ International Conference on Intelligent Robots and Systems (IROS '04, 2004*, pp. 419–424.
- [12] B. K.P.Horn, "Closed-form solution of absolute orientation using unit quaternions," *Optical Society of America A*, vol. 4, Apr 1987.
- [13] J. W. Weingarten, G. Gruener, and R. Siegwart, "Probabilistic plane fitting in 3d and an application to robotic mapping," in *2004 IEEE International Conference on Robotics and Automation (ICRA 2004)*, 2004, pp. 927–932.
- [14] D. W. Marquardt, "An algorithm for least-squares estimation of nonlinear parameters," *SIAM Journal on Applied Mathematics*, vol. 11, no. 2, pp. 431–441, 1963.
- [15] M. Yamaoka, "Mobility robot," in *Spring Congress 2008, Society of Automotive Engineers of Japan*, 2008.
- [16] N. Tomokuni, M. Shino, and M. Kamata, "Improving stability for a two-leg-wheeled inverted-pendulum-type vehicle equipped with a slider," in *Proceedings of 17th Annual Conference on Japan Society of Mechanical Engineering, Transportation and Logistics Division*, 2008, pp. 373–376.
- [17] N. Hatao, R. Hanai, K. Yamazaki, and M. Inaba, in *Proceedings of 15th IEEE International Symposium on Robot and Human Interactive Communication (ROMAN2009)*, 2009.



Fig. 15. Experiment for Path Following by PMR